Clinical Neurophysiology 123 (2012) 1656–1661

Contents lists available at SciVerse ScienceDirect

Clinical Neurophysiology

journal homepage: www.elsevier.com/locate/clinph

Conductive neuromagnetic fields in the lumbar spinal canal

Senichi Ishii [a], Shigenori Kawabata [a,*], Shoji Tomizawa [a], Masaki Tomori [a], Kyohei Sakaki [a], Kenichi Shinomiya [a], Kensuke Sekihara [b], Tomoya Sato [b], Yoshiaki Adachi [c], Atsushi Okawa [a]

[a] Department of Frontier Surgical Therapeutics, Section of Orthopedic and Spinal Surgery, Division of Advanced Therapeutical Sciences, Graduate School of Tokyo Medical and Dental University, Tokyo, Japan
[b] Department of Systems Design and Engineering, Tokyo Metropolitan University, Hino, Tokyo, Japan
[c] Applied Electronics Laboratory, Kanazawa Institute of Technology, Kanazawa, Shikawa, Japan

ARTICLE INFO

Article history:
Accepted 23 December 2011
Available online 27 January 2012

Keywords:
Neuromagnetic field
Lumbar spine
Cauda equina

HIGHLIGHTS

- We used a superconducting quantum interference device fluxmeter developed for use with the spine to measure propagating neuromagnetic fields at the surface of the lower back after stimulation of tibial nerves at the ankle.
- We simultaneously measured cauda equina action potentials with an epidural catheter-type electrode to validate the accuracy of the neuromagnetic field measurements.
- This method provides a noninvasive functional examination tool for lumbar spine disease.

ABSTRACT

Objective: To measure neuromagnetic evoked fields in the lumbar spinal canal.
Methods: Using a newly developed superconducting quantum interference device (SQUID) fluxmeter, neuromagnetic fields of 5 healthy male volunteers were measured at the surface of the lower back after stimulation of the tibial nerves at the ankles. For validation, we inserted a catheter-type electrode percutaneously in the lumbar epidural space in 2 of the subjects and measured cauda equina action potentials after tibial nerve stimulation.
Results: Neuromagnetic fields propagating from the intervertebral foramina into the spinal canal were measured, and the latencies of the magnetic fields corresponded largely with those of the cauda equina action potentials.
Conclusions: We successfully measured ascending neuromagnetic fields originating at the nerve root and the cauda equina with high spatial resolution. Future studies will determine whether neuromagnetic field measurement of the lumbar spine can be a useful diagnostic method for the identification of the disordered site in spinal nerves.
Significance: We successfully measured neuromagnetic fields in the lumbar spinal canal, which have previously been difficult to verify. Future studies will determine whether neuromagnetic field measurement of the lumbar spine can be a useful diagnostic method for identifying disorders of spinal nerves.

1. Introduction

Among patients with lumbar spine disease, such as lumbar spinal canal stenosis, many show compression of the cauda equina at multiple levels in morphologic images. In addition, the nerve root often appears to be compressed not only inside the spinal canal but also in the intervertebral foramen or extraforaminally. It is difficult to diagnose nerve lesions in such patients with the use of imaging methods alone. Therefore, a method for the evaluation of nerve function with high spatial resolution would be helpful. Taniguchi and colleagues measured cauda equina action potentials (CEAPs) after stimulation of the tibial or peroneal nerve with a needle electrode inserted into yellow ligament and reported that diagnosis of lesions is possible (Taniguchi et al., 2005). However, this invasive procedure can only be performed under general anesthesia. Therefore, the development of a noninvasive method is desirable.

There are reports evaluating action potentials of the cauda equina and spinal cord from outside of the body (Cracco, 1973; Small and Matthews, 1984; Eisen, 1986), but detailed diagnosis of spinal

* Corresponding author. Address: 1-5-45 Yushima, Bunkyo-ku, Tokyo 113-8519, Japan. Tel.: +81 3 5803 5279; fax: +81 3 5803 5281.
E-mail address: kawabata.orth@tmd.ac.jp (S. Kawabata).

1388-2457/$36.00
doi:10.1016/j.clinph.2011.12.014

lesions remains difficult. It is thought that this is because spinal nerves are situated deep from the body surface and are surrounded by the osseous tissue of the spine. Magnetic fields resulting from electrical nerve activity are not affected by surrounding tissues. Neuromagnetic recording has theoretically greater spatial resolution than electrical recording (Trahms et al., 1989; Hashimoto et al., 1991, 1994; Fukuoka et al., 2002, 2004; Kawabata et al., 2002). Tomori et al. (2010) used neuromagnetic recording at the body surface in animals to diagnose spinal cord lesions. In addition, conduction delay and conduction block have been visualized in human cervical spine (Adachi et al., 2008; Sato et al., 2009); therefore, progress is being made in the diagnosis of cervical spinal lesions.

In the lumbar spine, recording of conductive evoked magnetic fields at the body surface after stimulation of the tibial nerve has been reported (Curio et al., 1995; Mackert et al., 1997, 2001a,b). Mackert et al. (1998) also reported that the propagating field signal disappears around the intervertebral foramen in patients with S1 radiculopathy, thereby showing the potential clinical application of magnetic field measurement in the lumbar spine. However, clear magnetic field waveforms were observed only up to the intervertebral foramen in these studies. Klein et al. (2006) reported that they could detect a propagating signal along the sciatic nerve and plexus lumbosacralis up to around the intervertebral foramen of L5, and they could also detect a stationary signal in the upper part of the lumbar region. However, the signals ascending along the spinal canal could not be observed clearly, that is, activity of the cauda equina could not be detected. Therefore, further improvements are necessary for the clinical application of nerve magnetic field measurement in the lumbar spine.

The aim of the present study was to measure neuromagnetic fields at the surface of the lower back after peripheral nerve stimulation of the lower extremity in healthy subjects with the use of a supine position-type superconducting quantum interference device (SQUID) fluxmeter developed for use with the spine. We also aimed to show that cauda equina action magnetic fields (CEAFs) can be recorded in detail at the body surface and that detailed analysis at the level of clinical application is possible in the lumbar spine.

2. Materials and methods

2.1. Measurement of CEAFs

The study protocol was approved by the Ethics Committee of Tokyo Medical and Dental University. Inside a magnetically shielded room, 5 volunteer male subjects, 21–32 years of age (mean 25.4 years), 163–189 cm in height (mean 171 cm), 54–76 kg in weight (mean 63.4 kg), without any neurologic deficit, were placed in a relaxed supine position (Fig. 1C). The right and left tibial nerves were electrostimulated transcutaneously at each ankle, alternately (4–17 Hz; monophasic square-wave pulses; 0.2–3 ms width; constant current of 5–17 mA, clearly above the motor threshold for each subject).

Magnetic signals were recorded at 35 or 40 points (Fig. 2) with a 105- or 120-channel SQUID biomagnetometer system (Kanazawa Institute of Technology, Kanazawa, Japan) (Fig. 1A and B). A vector-type SQUID sensor was assigned to each measurement point. Each sensor was equipped with 3 gradiometric pickup coils orthogonal to each other to enable simultaneous detection of 3 independent magnetic field components. The diameter and baseline length of the pickup coils were 16 and 68 mm, respectively (Adachi et al., 2008). The typical noise floor at 500 Hz was around 3 $fT/Hz^{0.5}$. The measurement area was centered at the spinous process of L4 and placed coplanar to the lower back (no distance between the body surface and the dewar surface). A band-pass filter of 100 or 500 Hz–5 kHz was applied to the SQUID signals. A total of 4000–6000 responses were recorded at a sampling rate of 40 kHz and averaged separately for left and right nerve stimulation.

We used a unit gain normalized minimum-norm (UGMN) filter method to estimate the current source. This is a spatial filtering technique used to reconstruct the current source (Sekihara et al., 2005; Sekihara and Nagarajan, 2008). With this method, we extracted data for the depth of the nerve pathway from the lateral X-ray image and set reconstruction points on the pathway. With the use of the magnetic field data from all measurement points, we can reconstruct the direction and intensity of the current source on each reconstruction point and can visualize the conductive direction, distribution, and temporal change of the current source. This method is suitable for the reconstruction of the signal source with length and extension. This is in comparison to the conventional equivalent dipole method, which reconstructs the signal to just 1–2 points. The propagation pathway of the estimated electrical currents was superimposed on lumbar spine X-rays.

2.2. Measurement of SEPs

For comparison, somatosensory evoked potentials (SEPs) in response to tibial nerve stimulation were recorded simultaneously with the use of surface electrodes placed over the T12, L3, and L5 spinous processes, ischial tuberocity, and popliteal fossa. A reference electrode was placed on the contralateral anterior superior iliac spine. A band-pass filter of 100 or 500 Hz–5 kHz was applied to the signals, and 2000 responses were recorded and averaged.

2.3. Measurement of CEAPs

Cauda equina action potentials were also recorded after tibial nerve stimulation in 2 subjects (subjects 4 and 5) with the use of a catheter electrode (Unique Medical Co., Tokyo, Japan) placed in the epidural space at the lumbar level. The distance between each recording point was 15 mm. A reference electrode was placed on the contralateral anterior superior iliac spine. Signals were filtered with a 100 Hz or 500 Hz–5 kHz band-pass filter, and 2000 responses were recorded and averaged.

3. Results

3.1. Measurement of CEAFs after stimulation of the tibial nerve

For all subjects, CEAFs could be recorded after tibial nerve stimulation (Fig. 3). The spike waves of the obtained magnetic fields showed biphasic configurations; the first deflection of magnetic signals on the left side of the assumed L5 and S1 nerves (dotted line in Fig. 3) was directed outward (amplitudes up to 30 fT), and that of the right side was directed inward (amplitudes up to 30 fT). The polarity reversed for the second deflection. The peak of the first magnetic signals emerged at 13.7–18.6 ms (average 15.3 ms), and the peak of the second magnetic signals emerged at 15.6–21.1 ms (average 17.6 ms). The peak-to-peak amplitude was 21–57 fT (mean 32.6 fT). These waves propagated in a caudal to cranial direction at a conduction velocity of 43.2–69.6 m/s, as calculated from the peak latency; these velocities were consistent with physiologic nerve conduction velocities.

The isomagnetic field maps of CEAFs showed a quadrupolar pattern (Fig. 4A). The intra-axonal currents flowed from the axon depolarization site in the opposite direction along the nerve. The leading and trailing intra-axonal currents generated the magnetic fields (Fig. 4B). The field generated by the leading intra-axonal currents directed outward from ventral to dorsal on the left side of the nerve and inward from dorsal to ventral on the right side of the nerve.

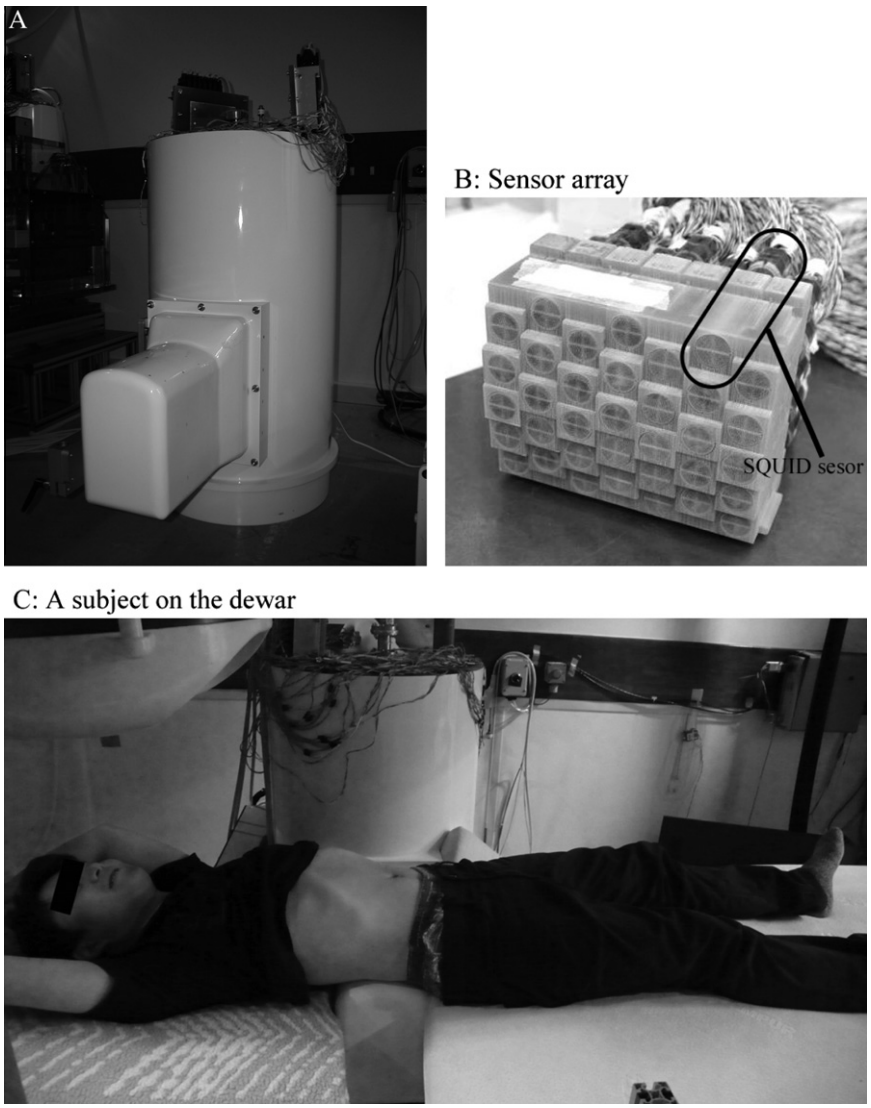

Fig. 1. (A) Vertical, cylinder-shaped cryostat with a sensor area protruding from the side. (B) An array of SQUID vector gradiometers with a 5 × 8 matrix-like arrangement. (C) The sensor surface is curved to fit to the lordosis of the subject's lumbar spine.

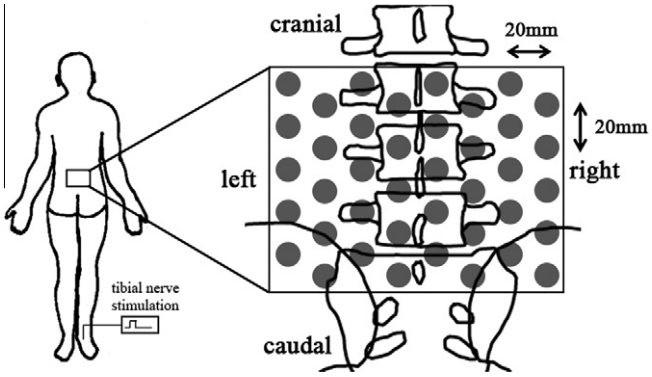

Fig. 2. CEAFs were recorded at 35 or 40 points over the skin surface after stimulation of the tibial nerve. Measurement points were arranged in a 5 × 7 or 5 × 8 matrix, and the distance between each point was 20 mm in both the longitudinal and lateral directions.

Depolarization was located between the cranial leading magnetic fields and the caudal trailing magnetic fields. This quadrupolar pattern is characteristic of the magnetic fields of nerve axonal activity. These quadrupolar fields emerged from the caudal area of the stimulated side, propagated to the center of the lumbar spine diagonally, and subsequently propagated cranially along the lumbar spinal canal at the L3–L5 level, according to the neural pathway.

3.2. Estimated current sources

The current sources of measured CEAFs were estimated by the UGMN filter method and visualized and superimposed onto X-ray images (Fig. 5). A conducting forward and backward current flow, according to the pathway from the nerve roots to the cauda equina, was recognized. In addition, volume currents surrounding intra-axonal currents were also observed. The forward current flow (leading axonal current flow) emerged at 13.5–17.5 ms (average 15.4 ms), and the backward current flow (trailing axonal current flow) emerged at 15.8–20.7 ms (average 18.3 ms). The conduction velocity of the current source waveform was 56.1–66.7 m/s, as calculated from the peak latency.

3.3. SEPs and CEAPs

Waveforms of SEPs recorded from the electrode placed on the L5 spinous process showed negative peaks in latency between

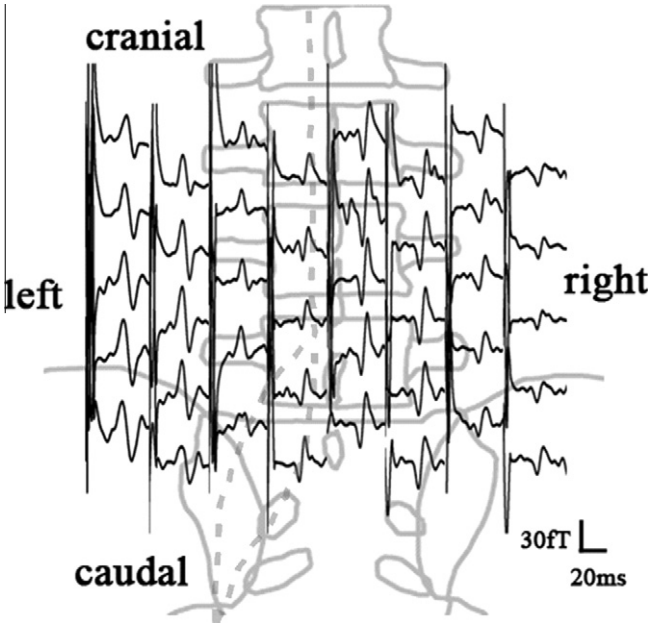

Fig. 3. Waveform arrangement of CEAFs after left tibial nerve stimulation based on measurement points. The waveforms are superimposed onto a schematic representation of the lumbar spine taken from the anterior–posterior view of an X-ray image. Signals above the baseline indicate outflux magnetic flow from ventral to dorsal, and signals below the baseline indicate influx magnetic flow from dorsal to ventral. The dotted line indicates the left L5 and S1 nerve roots and cauda equina ascending along the left side of the spinal canal, which we assumed.

14.9 and 19.1 ms, and the waveform recorded from the electrode placed on the L3 spinous process showed negative peaks in latency between 17.4 and 21.0 ms (Fig. 6A). Nerve conduction velocity between the L3 and L5 spinous processes was 32.4–357.6 m/s (mean 152.2 m/s), as calculated from the onset latency of the signal, and varied widely among subjects.

Waveforms of CEAPs recorded from the epidural electrodes showed propagation in the caudal to cranial direction (Fig. 6B). Nerve conduction velocity between L3 and L5 was 52.6–70.6 m/s (mean 64.5 m/s), as calculated from the onset latency.

The volume current components perpendicular to the nerve pathway were reconstructed from measured CEAFs by the UGMN filter method, and those waveforms estimated at 5 points in which epidural CEAPs were recorded were superimposed onto the CEAPs (Fig. 7). These waveforms corresponded almost exactly in both subjects in whom CEAPs were recorded.

4. Discussion

The magnetic fields identified in the present study showed a quadrupolar pattern characteristic of the magnetic fields of nerve axonal activity. In addition, the fields propagated along the spinal canal in a caudal to cranial direction, and the latencies of the magnetic fields corresponded with those of the epidural action potentials. These results indicate that the magnetic fields originated in the cauda equina inside the spinal canal and nerve roots.

Neuromagnetic recording has been reported for the purpose of functional diagnosis of nerve disorders such as cervical spondylotic myelopathy and lumbar spinal stenosis. With respect to cervical spine disease, we previously reported on the utility of neuromagnetic recording of spinal cord evoked fields after stimulation of the thoracic spinal cord, and a device for the identification of the disordered site has been developed (Adachi et al., 2006, 2007, 2008; Sato et al., 2009). In the lumbar spine, studies of neuromagnetic fields measured over the surface of the lower back after tibial nerve stimulation in humans have visualized the conduction of compound action potentials (Curio et al., 1995; Mackert et.al., 1997, 1998, 2001a,b). However, reports of propagation of the signal inside the spinal canal were not detailed.

Patients with lumbar spinal canal stenosis (LSCS) often have symptoms originating from central stenosis. For the accurate identification of the disordered site in patients with multiple stenoses in the lumbar spine, measurement of CEAFs inside the spinal canal is required. Clinically, L3/4 and L4/5 are often disordered (Hall et al., 1985). These disordered sites could be identified by observing signals originating in the cauda equina after tibial nerve stimulation. However, measurements of neuromagnetic fields in the lumbar spine have been difficult to obtain. The reason is considered to be that the cauda equina in the lumbar spine is thin and situated deep in comparison to the cervical spinal cord. In addition, the thoracic spinal cord can be stimulated by epidural electrodes when measuring spinal cord evoked fields (SCEFs) on the cervical spine, but in the lumbar spine, we can stimulate only a thin peripheral nerve. In fact, spinal cord evoked potentials (SCEPs) in response to stimulation of the thoracic spinal cord are approximately 10 μV (Tani et al., 1999), whereas CEAPs are approximately

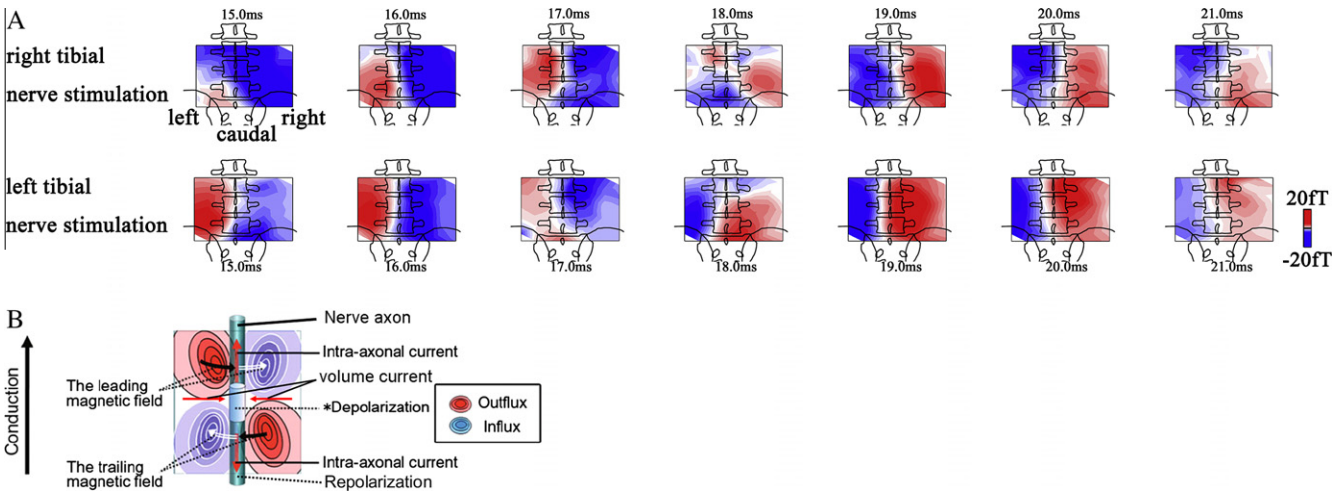

Fig. 4. (A) Isomagnetic field maps of CEAFs. Red indicates outflux magnetic flow from ventral to dorsal, and blue indicates influx magnetic flow from dorsal to ventral. The quadrupolar magnetic field propagated according to the neural pathway. (B) Characteristic quadrupolar pattern of axonal neuromagnetic fields.

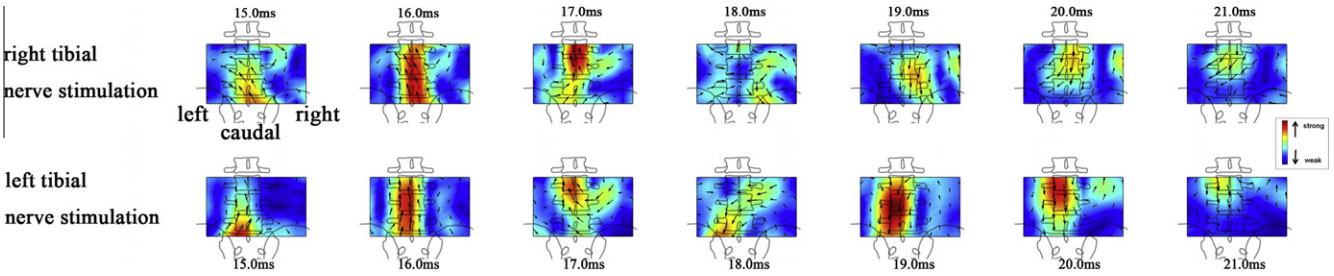

Fig. 5. Estimated current sources for CEAFs after tibial nerve stimulation. Small arrows indicate the current direction and intensity, and the color density indicates the current intensity. Propagating intra-axonal currents and volume currents were identified.

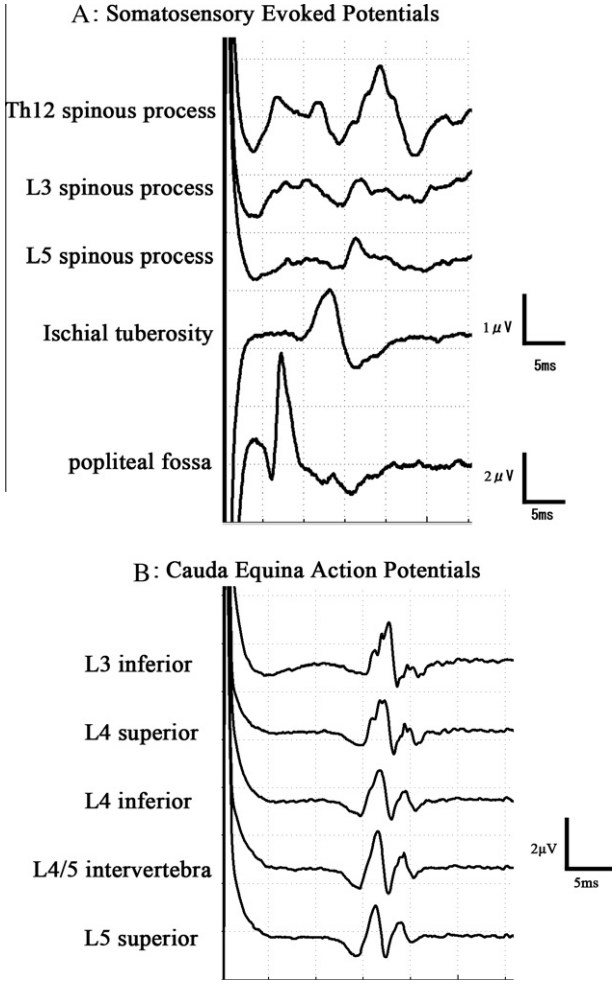

Fig. 6. (A) Waveforms of SEPs after left tibial nerve stimulation recorded on the T12, L3, and L5 spinous processes, and on the ischial tuberosity and popliteal fossa. The waveforms indicated propagation, though the conduction velocity varied widely among subjects. (B) Waveforms of CEAPs after left tibial nerve stimulation recorded from an epidural electrode placed at the level of L3–L5. Waveforms showed propagation in the caudal to cranial direction.

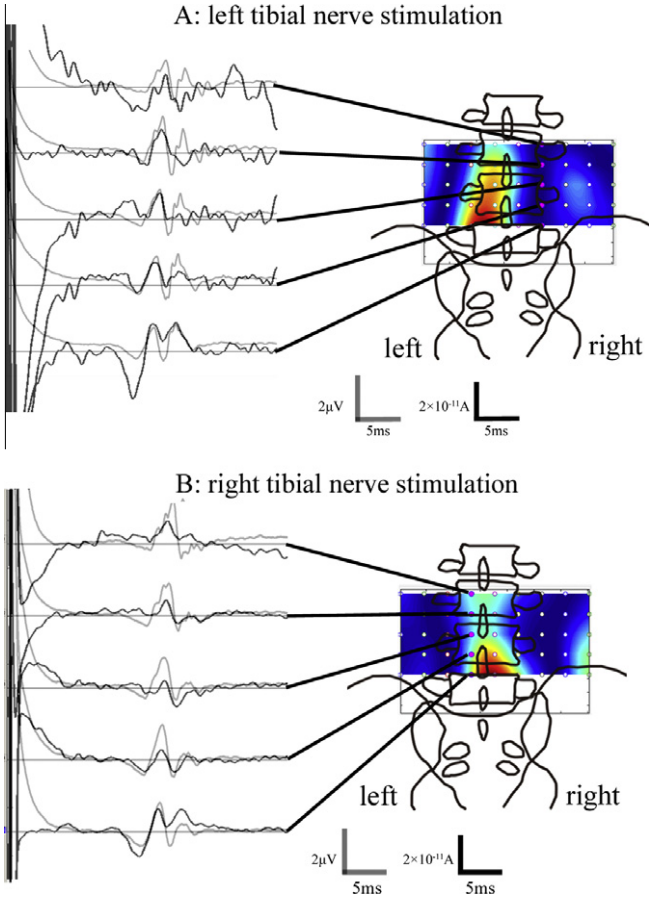

Fig. 7. Volume current components of current sources calculated from CEAFs (dark waveforms) were superimposed onto epidural CEAPs (light waveforms). (A) Left tibial nerve stimulation. (B) Right tibial nerve stimulation. The waveforms corresponded almost exactly.

2 μV, suggesting that evoked magnetic fields in the lumbar spine are also small.

In the present study, we detected signals ascending along the spinal canal and clearly visualized the signals in detail. Possible reasons why we were able to detect CEAFs include the following.

First, the subjects remained in a comfortable and stable supine position. Therefore, body movements and noise caused by muscle activity in response to stimulation were minimized. Second, fitting of the curved surface of the sensor to the lumbar lordosis minimized the distance between the sensors and nerves. In previous reports, the contact surface of the sensor was plane or concave and did not fit along the spine.

Furthermore, we were able to reconstruct the signal source originating in the cauda equina by analysis of the obtained signals with the UGMN filter method. This spatial filter method allowed us to reconstruct the current at any point. We found that CEAPs corresponded exactly with currents of components perpendicular to the nerve pathway reconstructed from magnetic data. Reconstructed currents perpendicular to the nerve pathway are considered to represent axonal depolarization (Tomori et al., 2010). We were able to demonstrate the high accuracy of measurement of neuromagnetic fields. This method may be useful for the accurate identification of the disordered site in spinal diseases. In addition,

given that we were able to measure neural activity around the intervertebral foramen, this method may be useful in the diagnosis of foraminal stenosis, which can be difficult.

Financial interests

The authors declare no financial interests.

Acknowledgements

The authors thank Mr. S. Fujii, Mr. R. Nakamura, and Mr. Y. Kawada of Tokyo Metropolitan University for their generous help and technical assistance.

References

Adachi Y, Miyamoto M, Kawai J, Uehara G. Measurement of spinal cord evoked magnetic fields by vector SQUID biomagnetometer. Electr Eng Jpn 2006;157:15–23.

Adachi Y, Kawai J, Uehara G, Miyamoto M, Tomizawa S, Kawabata S. A 75-ch SQUID biomagnetometer system for human cervical spinal cord evoked field. IEEE Trans Appl Supercond 2007;17:3867–73.

Adachi Y, Kawai J, Miyamoto M, Uehara G, Ogata H, Kawabata S. Multichannel SQUID system for measurement of spinal cord evoked magnetic field for supine subjects. J Phys Conf Ser 2008;97:012281.

Cracco RQ. Spinal evoked response: peripheral nerve stimulation in man. Electroencephalogr Clin Neurophysiol 1973;35:379–86.

Curio G, Mackert B-M, Burghoff M, Koetitz R, Drung D, Marx P. Neuromagnetic correlates of evoked somatosensory activity travelling through the lumbosacral cauda equina and thoracic spinal cord in man. In: Baumgartner G, Deecke L, Stroink C, Williamson SJ, editors. Biomagnetism: fundamental research and clinical applications. Amsterdam: Elsevier Science/IOS Press; 1995. p. 723–6.

Eisen AA. Noninvasive measurement of spinal cord conduction: review of presently available methods. Muscle Nerve 1986;9:95–103.

Fukuoka Y, Komori H, Kawabata S, Ohkubo H, Shinomiya K, Terasaki O. Imaging of neural conduction block by neuromagnetic recording. Clin Neurophysiol 2002;113:1985–92.

Fukuoka Y, Komori H, Kawabata S, Ohkubo H, Shinomiya K. Visualization of incomplete conduction block by neuromagnetic recording. Clin Neurophysiol 2004;115:2113–22.

Hall S, Bartleson JD, Onofrio BM, Baker Jr HL, Okazaki H, O'Duffy JD. Lumbar spinal stenosis. Clinical features, diagnostic procedures, and results of surgical treatment in 68 patients. Ann Intern Med 1985;103:271–5.

Hashimoto I, Odaka K, Gatayama T, Yokoyama S. Multichannel measurements of magnetic compound action fields of the median nerve in man. Electroencephalogr Clin Neurophysiol 1991;81:332–6.

Hashimoto I, Mashiko T, Mizuta T, Imada T, Iwase K, Okazaki H. Visualization of a moving quadrupole with magnetic measurements of peripheral nerve action fields. Electroencephalogr Clin Neurophysiol 1994;93:459–67.

Kawabata S, Komori H, Mochida K, Harunobu O, Shinomiya K. Visualization of conductive spinal cord activity using a biomagnetometer. Spine (Phila Pa 2002) 2002;27:475–9.

Klein A, van Leeuwen P, Hoormann J, Grönemeyer D. Magnetoneurographic registration of propagating magnetic fields in the lumbar spine after stimulation of the posterior tibial nerve. J Neural Eng 2006;3:125–31.

Mackert BM, Curio G, Burghoff M, Marx P. Mapping of tibial nerve evoked magnetic fields over the lower spine. Electroencephalogr Clin Neurophysiol 1997;104:322–7.

Mackert BM, Curio G, Burghoff M, Trahms L, Marx P. Magnetoneurographic 3D localization of conduction blocks in patients with unilateral S1 root compression. Electroencephalogr Clin Neurophysiol 1998;109:315–20.

Mackert BM, Burghoff M, Hiss LH, Trahms L, Curio G. Tracing of proximal lumbosacral nerve conduction – a comparison of simultaneous magneto- and electro-neurography. Clin Neurophysiol 2001a;112:1408–13.

Mackert BM, Burghoff M, Hiss LH, Nordahn M, Marx P, Trahms L, et al. Magnetoneurography of evoked compound action currents in human cervical nerve roots. Clin Neurophysiol 2001b;112:330–5.

Sato T, Adachi Y, Tomori M, Ishii S, Kawabata S, Sekihara K. Functional imaging of spinal cord electrical activity from its evoked magnetic field. IEEE Trans Biomed Eng 2009;56:2452–60.

Sekihara K, Sahani M, Nagarajan SS. Localization bias and spatial resolution of adaptive and non-adaptive spatial filters for MEG source reconstruction. Neuroimage 2005;25:1056–67.

Sekihara K, Nagarajan SS. Adaptive spatial filters for electromagnetic brain imaging. Berlin, Heidelber: Springer-Verlag; 2008.

Small M, Matthews WB. A method of calculating spinal cord transit time from potentials evoked by tibial nerve stimulation in normal subjects and in patients with spinal cord disease. Electroencephalogr Clin Neurophysiol 1984;59:156–64.

Tani T, Yamamoto H, Kimura J. Cervical spondylotic myelopathy in elderly people: a high incidence of conduction block at C3–4 or C4–5. J Neurol Neurosurg Psychiatry 1999;66:456–64.

Taniguchi S, Kawada T, Ushida T, Nagano Y, Ikemoto T, Tani T. Analysis of cauda equina action potentials recorded from the ligamentum flavum after peroneal nerve and tibial nerve stimulation during surgery for lumbosacral radiculopathies. Int Congr Ser 2005;1278:109–12.

Tomori M, Kawabata S, Tomizawa S, Ishii S, Enomoto M, Adachi Y, et al. Diagnosis of incomplete conduction block of spinal cord from skin surface using spinal cord evoked magnetic fields. J Orthop Sci 2010;15:371–80.

Trahms L, Erné SN, Tronteji Z, Curio G, Aust P. Biomagnetic functional localization of a peripheral nerve in man. Biophys J 1989;55:1145–53.